Published in final edited form as:
Free Radic Biol Med. 2009 November 15; 47(10): 1422–1431. doi:10.1016/j.freeradbiomed.2009.08.011.

Neurotoxic lipid peroxidation species formed by ischemic stroke increase injury

Stephanie L. H. Zeiger[a,b], **Erik S. Musiek**[c,d], **Giuseppe Zanoni**[e], **Giovanni Vidari**[e], **Jason D. Morrow**[c], **Ginger J. Milne**[c], and **BethAnn McLaughlin**[a,b,c,*]

[a] Department of Neurology, Vanderbilt University, Nashville, TN 37232

[b] Vanderbilt Kennedy Center, Vanderbilt University, Nashville, TN 37232

[c] Department of Pharmacology, Vanderbilt University, Nashville, TN 37232

[d] Department of Neurology, Hospital of the University of Pennsylvania, Philadelphia, PA 19104

[e] Department of Organic Chemistry, University of Pavia, Pavia 27100, Italy

Abstract

Stroke is the third leading cause of death in the United States yet no neuroprotective agents for treatment are clinically available. There is a pressing need to understand the signaling molecules which mediate ischemic cell death and identify novel neuroprotective targets. Cyclopentenone isoprostanes (IsoP), formed following free radical mediated peroxidation of arachidonic acid, are used as markers of stress but their bioactivity is poorly understood. We have recently shown that 15-A_{2t}-Isop is a potent neurotoxin *in vitro* and increases the free radical burden in neurons. In this work, we demonstrate that 15-A_{2t}-IsoP is abundantly produced in stroke infarcted human cortical tissue. Using primary neuronal cultures we found that minimally toxic exposure to 15-A_{2t}-IsoP does not alter ATP content, but in combination with oxygen glucose deprivation resulted in a significant hyperpolarization of the mitochondrial membrane and dramatically increased neuronal cell death. In the presence of Ca^{2+}, 15-A_{2t}-IsoP led to a rapid induction of the permeability transition pore and release of cytochrome *c*. Taken with our previous work, these data support a model in which ischemia causes generation of reactive oxygen species, calcium influx, lipid peroxidation and 15-A_{2t}-IsoP formation. These factors combine to enhance opening of the permeability transition pore leading to cell death subsequent to mitochondrial cytochrome *c* release. This data is the first documentation of significant 15-A_{2t}-IsoP formation following acute ischemic stroke and suggests addition of 15-A_{2t}-IsoP to *in vitro* models of ischemia may help to more fully recapitulate stroke injury.

Introduction

Stroke is the third leading cause of death in the United States and the leading cause of serious long-term disability. Each year there are approximately 700,000 new strokes, 88% of which are ischemic in nature [1]. The mechanisms by which cells die following ischemic injury have been intensively investigated for over 30 years. Core to the neurodegenerative process is the release of excessive glutamate resulting in overstimulation of receptors, ionic and energetic

*Correspondence should be addressed to: Dr. BethAnn McLaughlin, Vanderbilt University, MRB III Room 8141, 465 21st Avenue South, Nashville, TN 37232-8548 USA Tel: (615) 936-3847; Fax: (615) 936 3747; bethann.mclaughlin@vanderbilt.edu.

dysfunction which leads to oxidative and nitrosylative stress and protease activation [2]. In spite of this wealth of knowledge, we have been unsuccessful in designing therapeutics that block stroke induced death [3] suggesting that we need to more fully understand the biology of stroke to develop targets for drug design.

One of the least well understood components of the 'excitotoxic' cascade is the identification of discreet signaling molecules that contribute to oxidative injury. Excessive production of reactive oxygen species (ROS) cause cellular dysfunction and death, and an extensive literature supports a role for oxidative stress in the pathogenesis of stroke-induced neurodegeneration [4,5]. The extent of oxidative stress can be assessed using measures of injury such as F_2-IsoP formation. IsoPs are a family of prostaglandin-like molecules formed non-enzymatically as a result of free radical-mediated peroxidation of arachidonic acid. Measurement of F_2-IsoPs has been used as a 'gold standard' to measure cumulative oxidative damage from diet, exercise, renal, cardiac and recently neurological stress [6,7]. Indeed, F_2-IsoPs are elevated in a mouse model of stroke [8] and in a collaborative effort as part of the BEAT Stroke Study, we observed an increase in F_2-IsoP in the plasma of patients who experienced a stroke 6h-3days previously [9]. While the F_2-IsoPs have proven to be excellent markers of stress based on their stability, they are thought to be largely biologically inert and do not contribute to excitotoxicity [10]. F_2-IsoPs are not, however, the only products of the IsoP pathway.

Another set of IsoPs termed A_2/J_2- or cyclopentenone IsoPs, are formed alongside F_2-IsoPs *in vivo*, and are reactive electrophiles which form adducts with cellular thiols [11]. We have previously demonstrated that cyclopentenone IsoPs such as 15-A_{2t}-IsoPs have known bioactive properties and stimulate some of the same neurotoxic signaling events activated by stroke [10]. The mechanism of 15-A_{2t}-IsoP induced neurodegeneration in cultured neurons involves mitochondrial ROS production, glutathione depletion, 12-lipoxygenase activation, phosphorylation of ERK and $p66^{shc}$, and cleavage of caspases [12]. Based on these findings, we have hypothesized that cyclopentenone IsoPs, including 15-A_{2t}-IsoPs, are formed as a result of oxidative damage during ischemia/reperfusion, alter energetic status of cells by disruption of mitochondrial function and thus facilitate neuronal death. In spite of the similarities between the two stresses, we have previously not combined hypoxic injury with 15-A_{2t}-IsoPs to test this hypothesis.

In this current work, we have developed a new mass spectrometric method to directly evaluate A_2/J_2-IsoP formation in infarcted brain tissue from human ischemic stroke patients and found a significant increase in formation of these compounds within the injured brain. Furthermore, exogenous 15-A_{2t}-IsoP application was found to potentiate hypoxia induced neuronal cell death in our *in vitro* ischemia model. We show that although hypoxia induced a greater degree of mitochondrial hyperpolarization when 15-A_{2t}-IsoP is present, ATP generation was not further compromised. When mitochondria were incubated with15-A_{2t}-IsoP and Ca^{2+}, we observed a more rapid induction of the permeability transition pore and release of cytochrome *c* from the mitochondria. Taken together, this data suggests the presence of cyclopentenone IsoPs preceding ischemia/reperfusion injury may play an important role in determining a patient's outcome following a stroke.

Experimental methods

Materials and Reagents

15-A_{2t}-IsoP was generously provided by Drs. Giovanni Vidari and Giuseppe Zanoni (University of Pavia, Italy) while 15-deoxy-$\Delta^{12,14}$-prostaglandin J_2 (15d-PGJ_2) was obtained from Cayman Chemical Company (Ann Arbor, MI). Both compounds were stored at −80°C in ethyl acetate, then dried under nitrogen, resuspended in DMSO and added to media immediately before each experiment. All media and media supplements were from Gibco/BRL.

Antibodies for western blot analysis include cytochrome *c* 65981A (BD Biosciences) and anti-mouse IgG horseradish peroxidase conjugated secondary antibody (Cell Signaling Technology). Immunofluorescence antibodies include activated caspase-3 (Cell Signaling Technology, Inc.), 4′-6-diamidino-2-phenylindole (DAPI, Sigma) and cy2/cy3 fluorescent secondary antibodies (Cell Signaling Technology, Inc.). Tetramethyl rhodamine ethyl ester (TMRE) and carbonyl cyanide-p-trifluoromethoxyphenyl-hydrazon (FCCP) were obtained from Fluka Biochemika. The modular hypoxic chamber was purchased from Billups-Rothenberg Inc. Syto16 green fluorescent nucleic acid stain was obtained from Invitrogen. All other chemicals were from Sigma Chemical.

Human brain samples

Human post-mortem samples of frontal cortex were kindly provided from the Human Brain and Spinal Fluid Resource Center by Dr. Rashad Nagra of the Veterans Administration West Los Angeles Healthcare Center. Inclusion criteria for the stroke population were clinical and pathological diagnosis of focal ischemic stroke from clot or plaque occlusions of either the internal and external carotid arteries or the middle cerebral arteries. Exclusion criteria included any history of neurological disease including but not limited to Parkinson's disease, Alzheimer's disease, dementia, or known history of traumatic brain injury. The average patient age was 72.8±13.9 years, and the average post-mortem interval was 15.3±4.7 hours. Control samples were matched for age within 7 years and post mortem delay within 3 hours respectively and had no history of neurological diseases. Fresh frozen samples were dissected on dry ice and prepared for IsoP quantification in the manner described below.

Quantification of 15-A_2/J_2-IsoPs in human brain samples using LC/MS

Tissue samples (100–300mg) were homogenized in 5ml of ice-cold chloroform: methanol (2:1, v/v) containing butylated hydroxytoluene (0.005%) to prevent *ex vivo* autoxidation. [$^2H_4$]-PGA_2 (6ng) was then added to the homogenate as the internal standard. Esterified A_2/J_2-IsoPs in phospholipids were hydrolyzed using Apis melifera phospholipase A_2 to yield A_2/J_2-IsoP free fatty acids. The samples were then purified by extraction with a C_{18} Sep-Pak (Waters Corporation) that had been preconditioned by rinsing with methanol and distilled, deionized water (pH 3). After sample loading, the Sep-Pak was rinsed with 10mL each of water (pH 3) and heptane and the sample was eluted with ethyl acetate:heptane (1:1, v/v). The solvent was removed by evaporation under a stream of dry nitrogen and samples were resuspended in methanol:water (2:1, v/v) for LC/MS analysis.

Online LC was carried out using the ThermoFinnigan Surveyor MS Pump 2.0 equipped with a Luna C_{18} column (Phenomenex, 2.1mm × 50cm, 3μm particle size) utilizing a linear gradient mobile phase A: water/mobile phase B with 2mM ammonium acetate (95/5, v/v); mobile phase B: acetonitrile/methanol (95/5, v/v) with 2mM ammonium acetate with a flow rate of 200μL/min. A gradient of 80% to 50% mobile phase A over 18 minutes was used for the analysis of all samples. A Thermo Finnigan TSQ Quantum 1.0 SR 1 mass spectrometer was used for sample analysis. The mass spectrometer was operated using multiple reaction monitorin in the negative ion mode monitoring the transition of the precursor A_2/J_2-IsoP ion $[M-H]^-$ (*m/z* 333 to the 15-series specific product ion $[M–H\text{-}CH_2(OH)CH_2CH_2CH_2CH_2CH_3 – CO_2]^-$ (m/z 189). Analogous ions were monitored for the internal standard. Data acquisition and analysis was performed using *Xcaliber* software, version 1.3.

Cell culture

Cortical cultures were prepared from embryonic day 16 Sprague-Dawley rats as previously described [13]. Briefly, cortices were dissociated and the resultant cell suspension was adjusted to 770,000 cells/well (6-well tissue culture plates containing poly-L-ornithine-treated coverslips) in growth media. This media was composed of a volume to volume mixture of 80%

Dulbecco's Modified Eagle Medium (MEM), 10% Ham's F12-nutrients, 10% bovine calf serum (heat-inactivated, iron-supplemented; Hyclone) with penicillin, streptomycin, and 2mM L-glutamine. Glial cell proliferation was inhibited after two days in culture with 1–2μM cytosine arabinoside, after which the cultures were maintained in Neurobasal media (Gibco) containing 50X B27 supplement, penicillin and streptomycin. All experiments were conducted three weeks following dissection (21–25 days *in vitro*), when excitotoxicity is expressed fully in our system [14].

Neuronal oxygen glucose deprivation

In order to model ischemic cell death, primary neuronal cultures were exposed to oxygen glucose deprivation (OGD) for periods ranging from 0–90 minutes as previously described [12]. Mature neurons on glass coverslips were transferred to 35mm petri dishes containing glucose-free balanced salt solution (GBSS) with 10μM 15-A_{2t}-IsoP or DMSO. GBSS was first bubbled with nitrogen for 5 minutes to remove dissolved oxygen immediately prior to the addition of cells. Plates were then placed in an ischemia chamber (Billups-Rothberg), which was flushed with 95% nitrogen and 5% CO_2 for 5 minutes, then sealed and placed at 37°C for 25, 55, or 85 minutes for a total exposure time of 30, 60, and 90 minutes. OGD treatment was terminated by rinsing cells with MEM, followed by addition of MEM with 10mM Hepes, 0.001% BSA, and 2x N2 supplement (MEM/Hepes/BSA/2xN2) under normoxic conditions. 10μM 15-A_{2t}-IsoP or DMSO was present in the media during the ischemic exposure and the 24 hours following exposure.

Toxicity assays

Twenty four hours following the neuronal ischemic insult performed in the presence or absence of 10μM 15-A_{2t}-IsoP or vehicle (DMSO), cell death was assessed by visually inspecting the cells under phase bright microscopy as well as by using the lactate dehydrogenase (LDH) based *in vitro* toxicity kit (Sigma) according to the manufacturer's specifications. In order to account for minor variations in total LDH content across multiple dissections and platings, raw LDH values were normalized to the toxicity caused by the glutamate receptor excitotoxin, 100μM NMDA plus 10μM glycine, which is known to cause 100% cell death in this system [13]. All experiments were performed with an 'n' of four using cells derived from at least two independent original dissections. Statistical significance was determined by two-tailed *t*-test assuming unequal variances with $p < 0.05$.

ATP assays

Measurements of ATP content were performed 3 or 24 hours following 90 minute OGD in the presence or absence of 10μM 15-A_{2t}-IsoP or DMSO. Each coverslip was moved to a new plate containing 300μl of Cell Lysis reagent from the ViaLight® Plus Kit (Cambrex Bio Science). After ten minutes, 80μl of cell lysate was added to each well of a 96 well white plate with a transparent bottom followed by the addition of 100μl of ATP monitoring reagent. Addition of this reagent leads to the formation of light from the interaction of the enzyme luciferase with ATP present in the cell and luciferin. The resulting bioluminescent measurements are linearly related to ATP concentration and were taken on a Spectrafluor Plus plate reader (Tecan) following a two-minute incubation using an integration time of 1000ms and gain of 150. Measurements were obtained in duplicate for each sample and normalized for protein levels following a protein assay. ATP levels are expressed as the mean from three independent experiments ± standard error mean (S.E.M). Statistical significance was determined by two-tailed *t*-test assuming unequal variances with $p < 0.05$.

Tetramethylrhodamine ethyl ester (TMRE) measurement of mitochondrial membrane potential

All imaging was performed on an Axiovert 200 microscope fitted with a LD Plan-Neofluar 20x objective, an Axiocam MRm camera with 1388 × 1040 pixel resolution, a HBO 103 W/2 mercury short-arc lamp, and the Axiovision 4.5 software package (Carl Zeiss Inc.). For measurement of TMRE, cells were imaged using an excitation BP 546/12 and emission LP 590 filter set. For measurement of Syto 16, cells were imaged using an excitation BP 470/20 and emission BP 505–530 filter set.

Mitochondrial membrane potential ($\Delta\psi$) was assessed using a modification of the method previously described by Chan *et al* [15]. Following OGD, the coverslips were transferred to a 24 well plate containing 1mL of a warm (37°C) 50nM TMRE solution in MEM/Hepes/BSA/2xN2, plus either 15-A_{2t}-IsoP (10μM) or DMSO. Cells were incubated in the TMRE solution for 20 minutes at 37°C and 5% CO_2. After incubation, cells were rinsed twice with 37°C phosphate buffered saline solution (PBS) by removing half of the solution and adding 1mL of PBS. The remaining PBS was removed and replaced with 1mL of 37°C MEM/Hepes/BSA/2xN2 and fluorescent images were obtained by exciting TMRE at 555nm with emission detection at 590nm.

Because fluorescent indicators of $\Delta\psi$ cannot be readily calibrated in intact cells due to possible changes in plasma membrane potential [16–18], we used relative fluorescence changes to monitor $\Delta\psi$ as previously described [19]. The uncoupler FCCP was used to collapse $\Delta\psi$ and scale TMRE signal. After the initial imaging, MEM/Hepes/BSA/2xN2 was removed from each well of the 24 well plates by suction and 1mL of MEM/Hepes/BSA/2xN2 containing 10μM FCCP and 0.5μM Syto 16 green fluorescent nucleic acid stain was added. After five minutes, the FCCP solution was removed and the cells were rinsed with 1mL of 37°C PBS. The remaining PBS was removed and replaced with 1mL of 37°C MEM/Hepes/BSA/2xN2. Cells were then re-imaged for measurement of TMRE. Each field taken for measurement of TMRE was normalized with an accompanying Syto 16 measurement [20].

Image quantification

Cellular uptake of TMRE was quantified through the analysis of the gray scale histogram profile of each neuron in a field, with 5–15 neurons per field, using Adobe Photoshop CS2. To subtract background and account for variability in the number of mitochondria in each neuron, the mean pixel histogram value for each neuron was divided by the average mean pixel histogram value of an entire field from the same coverslip exposed to FCCP. For each experimental group the uptake of TMRE was expressed as the mean ± S.E.M of the neuron/FCCP pixel value ratio for all coverslips in that experimental group. Statistical significance was determined by two-tailed *t*-test assuming unequal variances with $p < 0.05$

Mitochondrial preparation

For biochemical assays of intact mitochondria, homogenates were made from Sprague-Dawley rat liver as previously described [21–23]. Briefly, liver was dissected, weighed and washed in 10ml cold PBS. The sample was homogenized using a dounce homogenizer in ice cold isolation media (250mM sucrose, 10mM Tris, 2mM EGTA, pH 7.4; 10mL/g of tissue). To remove intact cells and debris, the homogenate was spun at 500*g* for 10 minutes at 4°C followed by centrifugation of the resulting supernatant at 9400*g* for 10 minutes. The pellet was then washed, resuspended in EGTA-free isolation media and centrifuged 10 minutes more at 9400*g*. Following addition of 3mls of EGTA-free media, protein concentration was determined using the BCA protein assay.

Mitochondrial permeability transition pore assay

Opening of the mitochondrial permeability transition pore (PTP) was assayed spectrometrically using a light scattering assay as previously described [22,24,25]. Mitochondria (1 mg) were suspended in 1 ml of assay buffer (40mM Hepes, 195mM mannitol, 25mM sucrose, 5mM succinate, 1μM rotenone, pH 7.2) containing 10μM DMSO, varying concentrations of 15-A_{2t}-IsoP (1–40μM), or 10μM 15d-PGJ_2. Following a 2 minute equilibration period, $CaCl_2$ (20–80μM) was added and absorbance (535nM) was measured for 20 minutes at 37°C. Lag time before onset of swelling was measured by determining the time when the maximum rate of change in absorbance was evident following Ca^{2+} addition. For 15-A_{2t}-IsoP, 15d-PGJ_2 and DMSO comparison, lag time was normalized to DMSO in the presence of Ca^{2+} lag time. Data represents the mean from at least three independent experiments ± S.E.M. Statistical significance was determined by two-tailed *t*-test assuming unequal variances with $p < 0.05$

Cytochrome c release

During the PTP experiments, cytochrome *c* release was assessed following addition of cyclosporin A (5μM) and EGTA (1mM) to the mitochondrial suspension five minutes following Ca^{2+} addition to prevent further swelling [24,26]. The supernatant and mitochondrial pellet fractions were collected following centrifugation at 14000*g* for 5 minutes. Supernatants were further concentrated 20-fold by ultrafiltration using Microcon Ultracel YM-10 centrifugal filters. For western blot analysis, the eluate was resuspended in an equal volume of Laemmli sample buffer (Bio-Rad) which included a 1:20 dilution of β-mercaptoethanol.

Western blot analysis

Equal protein concentrations as determined by BCA protein assay were separated using Criterion Tris-HCl gels (Bio-Rad). Proteins were then transferred to polyvinylidene difluoride membranes (Amersham Biosciences) and blocked in methanol for five minutes. Following 10 minutes drying, the membranes were incubated overnight with cytochrome *c* antibody in 5% non fat dry milk in Tris buffered saline containing 0.1% Tween-20 (TBS-Tween). Membranes were washed three times with TBS-Tween, and incubated with horseradish peroxidase conjugated secondary antibody for one hour. Following three additional washes in TBS-Tween, the protein bands were visualized using Western Lightning© chemiluminsecence reagent plus enhanced luminol reagents (PerkinElmer Life Science). The NIH Image J analysis program was used to quantify the cytochrome *c* western band intensity as we have previously described [13]. The 15-A_{2t}-IsoP and 15d-PGJ_2 induced changes in cytochrome *c* intensities were normalized to the intensity obtained for DMSO and data represent the fold increase over this vehicle control. All data points represent at least three independent experiments ± standard error mean. Statistical significance was determined by two-tailed *t*-test assuming unequal variances with $p < 0.05$

Immunofluorescence and quantification of activated caspase 3 containing cells

Six hours following exposure to 15-A_{2t}-IsoPs or DMSO with or without 90 minute OGD, cultures were fixed in 10% formaldehyde for 20minutes, then rinsed with PBS, permeabilized with 0.1% Triton X-100, and blocked for 1hour with 1% bovine serum albumin diluted in PBS. Coverslips were then incubated overnight at 4°C in anti-activated caspase-3 primary antibody, washed with PBS for a total of 20minutes and incubated in cy-2 or cy-3-labeled secondary antibodies for 1hour. Cells were then washed and stained with 1.4 μm DAPI for 10 minutes, followed by further washes. Coverslips were mounted on microscope slides, and fluorescence was visualized with a Zeiss Axioplan microscope [12]. The percentage of cells containing activated caspase was determined by counting the number of activated caspase immunostained cells and dividing by the total number of DAPI stained cells for five different fields of view.

All data points represent the average ± S.E.M. from three independent experiments. Statistical significance was determined by two-tailed *t*-test assuming unequal variances with $p < 0.05$

Results

IsoP is increased following human ischemic stroke

We have previously demonstrated that 15-A_{2t}-IsoP is a potent inducer of neuronal apoptosis when applied to primary neurons in culture, and exacerbates oxidative glutamate toxicity *in vitro* [12]. While high levels of glutamate have been linked to stroke injury [27–31] and lipid peroxidation has been documented following stroke like injuries [32,33,34], the importance of 15-A_{2t}-IsoP formation in cell death following stroke induced injury has not been previously explored. To this end, we obtained fresh frozen post-mortem human cortical brain tissue samples from infarcted regions of cortex from stroke patients or from matched areas of cortex from neurologically intact control patients in order to determine if these bioactive products are formed following stroke.

Our prior work assessing CNS formation of cyclopentenone IsoPs employed a mass spectrometric assay which quantified all cyclopentenone IsoP isomers together and was not sensitive enough to apply to small samples [12]. For this work, we developed a new liquid chromatography-tandem mass spectrometry (LC-MS/MS) methodology far more sensitive and specific than our previous gas chromatography-MS assay which can quantify specific IsoP isomers such as 15-A_2/J_2-IsoPs. We employed this assay to quantify levels of esterified 15-A_2/J_2-IsoPs which serve as indices of cyclopentenone IsoP formation, in our human stroke brain and control samples. In all control brain samples, levels of 15-A_2/J_2-IsoPs were near the limit of detection of our assay, which can detect quantities as low as ~0.2ng/g of brain tissue. In all six human stroke specimens, a pronounced 15-A_2/J_2-IsoP peak was readily apparent. Quantification via stable isotope dilution using a deuterium-labeled PGA_2 as the internal standard revealed a 4-fold increase in 15-A_2/J_2-IsoP levels in stroke samples compared to controls (Fig. 1).

While the chromatographic nature of the A_2/J_2 compounds under the conditions required for LC/MS analysis allows unprecedented levels of detection, it is, however, not possible to further separate the 8 different stereoisomers of the 15-A_2 and 15-J_2-IsoPs from each other. Other methods with far lower sensitivity, such as normal phase LC can achieve this end, but this separation methodology is not compatible with our electrospray ionization MS methodology. Based upon our experience with the oxidation of arachidonic acid *in vitro* and *in vivo*, it is highly unlikely that the peaks detected in the mass spec are a result of just the 15-A_2- or just the 15-J_2-IsoPs as they would be expected to be formed in equal abundance [11,35].

15-A_{2t}-IsoP in combination with OGD enhances neuronal toxicity

We next assessed if a sublethal dose of 10μM 15-A_{2t}-IsoP could potentiate the injury of oxygen glucose deprivation. We, and others, use mature primary neuronal cultures exposed to OGD to model ischemia/reperfusion injury associated with stroke [13,36,37]. Like *in vivo* tissue, loss of oxygen and glucose leads to rapid loss of cellular membrane potential, release of cytokines and excitotoxins and substantial oxidative stress [2].

Using this model, we evaluated neuronal toxicity following OGD for 30, 60, or 90 minutes in the presence or absence of 15-A_{2t}-IsoP. Following treatment, cells were returned to normal growth media and cell death was assessed 24hrs later. We found increased cell death in neurons exposed to 90 minute OGD treatment which caused 39% neuronal death (Fig. 2). Addition of the non-toxic dose of 10μM 15-A_{2t}-IsoP in combination with OGD for 90 minutes significantly

increased cell death, elevating total cell death under these conditions to approximately 70% (Fig. 2).

15-A_{2t}-IsoP does not alter ATP homeostasis

Previously, we demonstrated that higher concentrations of 15-A_{2t}-IsoP activated cell death via a pathway requiring mitochondrial ROS production and that cell injury was abated in the presence of the mitochondrial uncoupler FCCP. This suggests that either removing mitochondrial free radicals decreased death or that 15-A_{2t}-IsoP may alter the energetic status of neurons at the level of either the Krebs cycle or electron transport chain [12].

To test the contribution of 15-A_{2t}-IsoP to energetic dysfunction, we first measured the ATP content of neurons 3 and 24 hours following exposure to OGD in the presence or absence of 10μM 15-A_{2t}-IsoP. We observed a dramatic loss of energetic stores 3 hours following exposure to 90 minutes of OGD, which did not recover even 24 hours later (Fig. 3). The failure of 15-A_{2t}-IsoP to significantly alter ATP content beyond that induced by OGD at either 3 or 24 hours suggests that this level of 15-A_{2t}-IsoP does not further inhibit electron transport or Krebs cycle production of reducing equivalents necessary for ATP production.

Increased hyperpolarization of the mitochondrial membrane potential occurs in the presence of 15-A_{2t}-IsoP and hypoxia

A variety of molecular, ionic and energetic mechanisms converge to determine the electrochemical gradients of the mitochondrial membrane potential (MMP). As the MMP is imperative in regulating the activation of apoptotic signaling pathways, we wanted to determine if 15-A_{2t}-IsoP altered neuronal mitochondrial polarization using the fluorescent indicator cell permeable positively charged molecule TMRE which rapidly accumulates in mitochondria as a function of the membrane potential [19].

Neurons were easily identified by positive Syto 16 staining and had well defined somas and processes (Fig. 4 panel A). Following either OGD or 15-A_{2t}-IsoP exposure for 90 minutes, there was a significant decrease in the intensity of the TMRE staining (Fig. 4, panels B and C) with only a fewer intensely labeled cells (arrowheads). Surprisingly, the combination of OGD and 15-A_{2t}-IsoP resulted in an increase in mitochondrial sequestration of TMRE (Fig. 4, panel D) relative to either compound alone. Given that TMRE has very limited interactions with mitochondrial structures [38], the most likely interpretation of this data is that mitochondria become hyperpolarized immediately after the paired insults.

While some teams have observed increased intensity of polar mitochondrial dyes as a function of mitochondrial biogenesis, the time course of these observations is on the orders of days and not likely a factor in interpreting the changes observed during the short time frame of these experiments (<3 hours from insult to recording) [39]. To ensure we did not have a biogenesis artifact, we did, however, perform fluorescent readings of neurons exposed to these conditions and loaded with the Mitotracker Green FM dye which accumulates in mitochondria regardless of mitochondrial coupling [40]. We found no difference in fluorescent intensity resulting from OGD, 15-A_{2t}-IsoP or a combination of the two conditions at this time point (data not shown) suggesting that the changes in TMRE represent mitochondrial hyperpolarization rather than increased numbers of mitochondria.

15-A_{2t}-IsoP enhances PTP opening in the presence of Ca^{2+}

The mitochondrial membrane potential hyperpolarizes with extrusion of protons from the matrix allowing the cytochromes within the electron transport chain to become more reduced [12]. Moreover, hyperpolarization enhances the electrochemical gradient for Ca^{2+} transport into the mitochondria which can adversely affect neuronal viability [41]. Ca^{2+} overload in

stroke and other pathological conditions leads to opening of the permeability transition pore (PTP) within the inner mitochondrial membrane and the subsequent release of pro-apoptotic proteins [28,42–45]. Both the isomeric bioactive prostaglandin 15-deoxy-$\Delta^{12,14}$-prostaglandin J_2 (15d-PGJ_2), a cyclooxygenase-derived enzymatic product of arachidonic acid peroxidation, and arachidonic acid itself have both been shown to open the PTP and lead to the release of cytochrome *c* [24,46].

To determine if 15-A_{2t}-IsoP has a similar effect on the PTP, we exposed purified liver mitochondria to 10μM DMSO, 15-A_{2t}-IsoP, or 15d-PGJ_2 in the presence or absence of Ca^{2+} and sphectrometrically monitored opening of PTP. Neither DMSO, 15-A_{2t}-IsoP, nor 15d-PGJ_2 promoted swelling of the mitochondria on their own throughout the 30 minute measurement window. However, in the presence of Ca^{2+}, 15-A_{2t}-IsoP led to a 1.5 fold increase in the onset of swelling compared to DMSO alone (Fig. 5 panels A, B), but had a lower effect than 15d-PGJ_2. The effect of 15-A_{2t}-IsoP was concentration dependent as the time of opening and magnitude was enhanced with increased levels of IsoP (Fig. 5 panels C, D).

Cytochrome c release from mitochondria occurs following treatment with 15-A_{2t}-IsoP and Ca^{2+}

We next evaluated if cytochrome *c* was released from the purified mitochondria exposed to either 15d-PGJ_2 or 15-A_{2t}-IsoP using western blot analysis of the supernatant fraction following treatment. Based on the normalized band intensity, we observed that both 15-A_{2t}-IsoP and 15d-PGJ_2 induced substantial mitochondrial release of cytochrome *c* in the presence of calcium and a significant increase compared to DMSO in the absence of calcium (Fig. 6 panels A, B).

Previously, we have demonstrated that 15-A_{2t}-IsoP treatment at higher concentrations (30μM) led to activation of caspase -3 and apoptotic neuronal death [12]. As PTP opening has been linked to both necrotic and apoptotic death while cytochrome *c* release is known to activate the apoptosome [42,45,47–49], we next evaluated if the combination of OGD and 15-A_{2t}-IsoP similarly led to an increase in apoptotic death. Six hours following treatment of neurons with DMSO or 15-A_{2t}-IsoP with or without 90 minute OGD, we stained for cleaved caspase 3 and quantified the percentage of total cells demonstrating activated caspase 3. We observed a substantial increase in activated caspase 3 containing cells following OGD and 15-A_{2t}-IsoP exposure compared to OGD alone (Fig. 6 panel C). Taken together, this data suggests increased cytochrome *c* release in the presence of 15-A_{2t}-IsoP and OGD temporally coincides with the opening of the PTP and results in apoptotic signaling.

Discussion

The isoprostanes are a family of prostaglandin-like molecules which are formed non-enzymatically in all cell membranes as a result of free radical-mediated peroxidation of arachidonic acid. Numerous studies have demonstrated increased F_2-IsoP levels in neurodegenerative diseases and while F_2-IsoP itself is not bioactive, cyclopentenone IsoPs which are also formed *in vivo* are reactive electrophiles [6,10–12,50,51]. These compounds, also known as A_2/J_2-IsoPs, readily form Michael adducts with cellular thiols, including those found in cysteine residues and in glutathione [11].

We have previously shown that cyclopentenone IsoPs are formed in animals when exposed to oxidizing conditions and that these compounds potently induce apoptosis when applied to primary neuronal cultures [12]. This current work is the first demonstration that the reactive cyclopentenone A_2/J_2-IsoPs are formed in the CNS in patients who have suffered an ischemic stroke. Our data also support a model in which the specific cyclopentenone 15-A_{2t}-IsoP potentiates stroke induced injury in neurons via a prodeath mitochondrial pathway.

Neuronal mitochondrial function is an essential determinant of cell fate following injury and the balance of energetic signaling and molecular cues to determine if hypoxic, oxidative, and hypoglycemic injury is lethal [2]. Alterations of mitochondrial membrane potential, calcium dysfunction, and decisions to release pro-apoptotic factors, which activate transcriptionally dependent and independent signaling, place mitochondria at the heart of the response to neurodegeneration [52]. The enhanced extrusion of protons upon a combined exposure of OGD and 15-A_{2t}-IsoP in our *in vitro* model of ischemic injury suggests that when faced with the paired insults of ischemia and lipid peroxidation, neurons undergo a rapid and intense change in mitochondrial polarity. Indeed, acute mitochondrial hyperpolarization has been observed in response to many neurotoxic stressors as a means to drive aerobic ATP production by increasing the proton gradient responsible for oxidative phosphorylation [53–55]. In the current set of experiments, the presence of 15-A_{2t}-IsoP did not, however, have further detrimental effects on ATP production compared to ischemia alone indicating 15-A_{2t}-IsoP does not impact net energetic status.

Both hypoxia and ischemia have been linked to opening of the outer mitochondrial membrane which would lead to an extrusion of protons [56–58]. This phenomenon would result in hyperpolarization similar to our TMRE results following 15-A_{2t}-IsoP and OGD treatment. Similar to previous work demonstrating that products of fatty acid oxidation induce PTP opening and cytochrome *c* release [24,46], we found that the non-enzymatically derived lipid oxidation product 15-A_{2t}-IsoP led to a more rapid opening of the PTP and cytochrome *c* release in the presence of Ca^{2+}. Taken with the increased activation of caspase 3 following OGD and 15-A_{2t}-IsoP exposure, we believe these events culminate into the activation of apoptotic death pathways.

Given the ability of 15-A_{2t}-IsoP to adduct to thiol residues, we hypothesize that this cyclopentenone IsoP may be interacting with PTP proteins to enhance pore sensitivity to Ca^{2+}. This hypothesis is supported by a proteomics analysis which identified several proteins in isolated mitochondria that are directly modified by 15d-PGJ_2 including ATP synthase and adenine nucleotide translocase (ANT), two proteins important for pore formation [24,59–61]. In particular, ANT has a critical cysteine residue that is responsible for adenine nucleotide inhibition of PTP and important for binding of cyclophilin-D for pore formation that is susceptible to oxidative stress [62,63].

While both 15-A_{2t}-IsoP and 15d-PGJ_2 induce PTP opening, PGJ_2 activates the PPAR nuclear receptor and was shown to be neuroprotective following glutamate induced toxicity in cortical cultures [12,24,50,64]. Indeed, PGJ_2 increased glutathione levels through upregulation of electrophile response element containing genes such as glutathione synthetase and glutamate-cysteine ligase [64]. This is in contrast to 15-A2t-IsoP which we have demonstrated decreases glutathione levels in cortical neurons [12]. Thus, 15-A_{2t}-IsoP's ability to enhance PTP opening may be a consequence of glutathione depletion resulting in increased ROS which then adduct to the critical cysteines in PTP pore proteins. This could explain the slower kinetics for PTP opening compared to 15d-PGJ_2. Alternatively, the difference may be due to the increased potency of Michael addition reactions for 15d-PGJ_2's two electrophile β-carbons versus 15-A_{2t}-IsoP's single electrophile β-carbon.

In conclusion, the treatment of ischemic stroke remains one of the most challenging areas of medicine today. At present, only one agent is approved (Alteplase, rt-PA), and for only a brief window of time (onset of symptoms less than three hours) [65]. Moreover, we recognize that the models of stroke induced death fail to recapitulate many aspects of the clinical realities of ischemia. As we seek to refine both *in vivo* and *in vitro* stroke models to more fully identify potential molecules to alter the fate of ischemically injured cells, understanding bioactive lipid products as discreet mediators of stress and more fully capturing the *in vivo* lipid environment

in our cell culture models is essential to developing appropriate therapies [66]. To this end, we believe evaluation of 15-A_{2t}-IsoP formation during stroke and consideration of inclusion of pathophysiologically relevant levels of 15-A_{2t}-IsoP and other lipids to *in vitro* stroke models may allow us to more fully recapitulate stroke induced injury. This importance of lipid bioactivity is further highlighted by the fact that strong risk factors associated with stroke including hypertension, history of transient ischemic attacks, diabetes, high cholesterol and arthrosclerosis demonstrate increased IsoP formation [67,68]. As neuronal toxicity is enhanced by 15-A_{2t}-IsoP during hypoxia, it will be of interest to determine if baseline levels of cyclopentenone IsoPs before stroke directly impact morbidity and mortality.

Acknowledgments

The authors wish to thank Dr. Rashad Nagra for providing human tissue samples, Dr. Alessio Porta for her part in synthesizing 15-A_{2t}-IsoP and Clayton Wilburn for his analyzing TMRE staining. We also appreciate the thoughtful suggestions of Mr. Joshua Parlaman, Drs. Joshua Brooks, Gregg Stanwood and Laura Lillien when preparing this manuscript. This work was supported by NIH grants NS050396 and the training grant MH065215. Statistical analysis was provided with the support of the NICHD Grant P30HD15052. Support for ESM was provided by a grant from the PhRMA foundation.

List of abbreviations

IsoP
: isoprostanes

GBSS
: glucose-free balanced salt solution

ROS
: reactive oxygen species

LDH
: lactate dehydrogenase

BSA
: bovine serum albumin

TMRE
: Tetramethyl rhodamine ethyl ester

CNS
: central nervous system

LC
: liquid chromatography

MS
: mass spectrometry

OGD
: oxygen glucose deprivation

$\Delta\psi$
: mitochondrial membrane potential

FCCP
: carbonyl cyanide-p-trifluoromethoxyphenyl-hydrazon

References

1. American-Heart-Association, American Heart Association. Heart Disease and Stroke Statistics — 2005 Update. 2005
2. Lipton P. Ischemic cell death in brain neurons. Physiological Reviews 1999;794:1431–568. [PubMed: 10508238]
3. Ginsberg MD. Neuroprotection for ischemic stroke: Past, present and future. Neuropharmacology 2008;553:363. [PubMed: 18308347]
4. Coyle JT, Puttfarcken P. Oxidative stress, glutamate, and neurodegenerative disorders. Science 1993;2625134:689–95. [PubMed: 7901908]
5. Chan PH. Reactive oxygen radicals in signaling and damage in the ischemic brain. Journal of Cerebral Blood Flow & Metabolism 2001;211:2–14. [PubMed: 11149664]
6. Roberts LJ 2nd, Morrow JD. Products of the isoprostane pathway: unique bioactive compounds and markers of lipid peroxidation. Cell and Molecular Life Sciences 2002;595:808–20.
7. Morrow J, Hill K, Burk R, Nammour T, Badr K, Roberts ILJ. A Series of Prostaglandin F2-Like Compounds are Produced in vivo in Humans by a Non- Cyclooxygenase, Free Radical-Catalyzed Mechanism. Proceedings of the National Academy of Sciencesof the United States of America 1990;8723:9383–9387.
8. Marin JG, Cornet S, Spinnewyn B, Demerle-Pallardy C, Auguet M, Chabrier PE. BN 80933 inhibits F-2-isoprostane elevation in focal cerebral ischaemia and hypoxic neuronal cultures. Neuroreport 2000;116:1357–1360. [PubMed: 10817621]
9. Kelly PJ, Morrow JD, Ning M, Koroshetz W, Lo EH, Terry E, Milne GL, Hubbard J, Lee H, Stevenson E, Lederer M, Furie KL. Oxidative stress and matrix metalloproteinase-9 in acute ischemic stroke: the Biomarker Evaluation for Antioxidant Therapies in Stroke (BEAT-Stroke) study. Stroke 2008;391:100–4. [PubMed: 18063832]
10. Musiek ES, Milne GL, McLaughlin B, Morrow JD. Cyclopentenone eicosanoids as mediators of neurodegeneration: A pathogenic mechanism of oxidative stress-mediated and cyclooxygenase-mediated neurotoxicity. Brain Pathology 2005;152:149–158. [PubMed: 15912888]
11. Chen Y, Morrow JD, Roberts LJ. 2nd, Formation of reactive cyclopentenone compounds in vivo as products of the isoprostane pathway. The Journal Of Biological Chemistry 1999;27416:10863. [PubMed: 10196163]
12. Musiek ES, Breeding RS, Milne GL, Zanoni G, Morrow JD, McLaughlin B. Cyclopentenone isoprostanes are novel bioactive products of lipid oxidation which enhance neurodegeneration. Journal Of Neurochemistry 2006;975:1301–1313. [PubMed: 16638022]
13. McLaughlin BA, Hartnett KA, Erhardt JA, Legos JJ, White RF, Barone FC, Aizenman E. Caspase 3 activation is essential for neuroprotection in ischemic preconditioning. Proceedings of the National Academy of Sciences of the United States of America 2003;1002:715–720. [PubMed: 12522260]
14. Sinor JD, Boeckman FA, Aizenman E. Intrinsic redox properties of N-methyl-D-aspartate receptor can determine the developmental expression of excitotoxicity in rat cortical neurons in vitro. Brain Research 1997;7472:297–303. [PubMed: 9046005]
15. Chan SL, Liu D, Kyriazis GA, Bagsiyao P, Ouyang X, Mattson MP. Mitochondrial Uncoupling Protein-4 Regulates Calcium Homeostasis and Sensitivity to Store Depletion-induced Apoptosis in Neural Cells. The Journal Of Biological Chemistry 2006;28149:37391–37403. [PubMed: 17035241]
16. Di Lisa F, Blank PS, Colonna R, Gambassi G, Silverman HS, Stern MD, Hansford RG. Mitochondrial membrane potential in single living adult rat cardiac myocytes exposed to anoxia or metabolic inhibition. Journal of Physiology (London) 1995;4861:1–13. [PubMed: 7562625]
17. Farkas DL, Wei MD, Febbroriello P, Carson JH, Loew LM. Simultaneous imaging of cell and mitochondrial membrane potentials [published erratum appears in Biophys J 1990 Mar;57 (3):following 684]. Biophysical Journal 1989;566:1053–1069. [PubMed: 2611324]
18. Solaini G, Sgarbi G, Lenaz G, Baracca A. Evaluating mitochondrial membrane potential in cells. Bioscience Reports 2007;271–3:11–21.
19. Lawrence CL, Billups B, Rodrigo GC, Standen NB. The KATP channel opener diazoxide protects cardiac myocytes during metabolic inhibition without causing mitochondrial depolarization or flavoprotein oxidation. British Journal of Pharmacology 2001;1343:535. [PubMed: 11588107]

20. Frey T. Nucleic acid dyes for detection of apoptosis in live cells. Cytometry 1995;213:265–74. [PubMed: 8582249]
21. Clark JB, Nicklas WJ. The metabolism of rat brain mitochondria. Preparation and characterization. The Journal Of Biological Chemistry 1970;24518:4724–31. [PubMed: 4393961]
22. Pon, LAaS; Eric, A. Methods in Cell Biology Mitochondria. In: Wilson, Paul LaM, editor. Mitochondria. Vol. 2. Vol. 80. San Diego: Elsevier; 2007.
23. Brookes PS V, Darley-Usmar M. Role of calcium and superoxide dismutase in sensitizing mitochondria to peroxynitrite-induced permeability transition. American Journal of Physiology Heart and Circulatory Physiology 2004;2861:H39–46. [PubMed: 12933349]
24. Landar A, Shiva S, Levonen AL, Oh JY, Zaragoza C, Johnson MS, Darley-Usmar VM. Induction of the permeability transition and cytochrome c release by 15-deoxy-Delta12,14-prostaglandin J2 in mitochondria. Biochemical Journal 2006;394(Pt 1):185–95. [PubMed: 16268779]
25. Speer O, Morkunaite-Haimi S, Liobikas J, Franck M, Hensbo L, Linder MD, Kinnunen PK, Wallimann T, Eriksson O. Rapid suppression of mitochondrial permeability transition by methylglyoxal. Role of reversible arginine modification. The Journal of Biological Chemistry 2003;27837:34757–63. [PubMed: 12815061]
26. Yang JC, Cortopassi GA. Induction of the mitochondrial permeability transition causes release of the apoptogenic factor cytochrome c. Free Radic Biol Med 1998;244:624–31. [PubMed: 9559874]
27. Skaper SD, Facci L, Strijbos PJLM. Neuronal Protein Kinase Signaling Cascades and Excitotoxic Cell Death. Annals of the New York Academy of Sciences 2001;9391:11–22. [PubMed: 11462762]
28. Kristian T, Siesjo BK. Calcium in ischemic cell death. Stroke 1998;293:705–18. [PubMed: 9506616]
29. Seki Y, Feustel PJ, Keller RW, Tranmer BI, Kimelberg HK. Inhibition of ischemia-induced glutamate release in rat striatum by dihydrokinate and an anion channel blocker. Stroke 1999;30:433. [PubMed: 9933284]
30. Lipton SA. Failures and Successes of NMDA Receptor Antagonists: Molecular Basis for the Use of Open-Channel Blockers like Memantine in the Treatment of Acute and Chronic Neurologic Insults. NeuroRx 2004;11:101–110. [PubMed: 15717010]
31. Endres M, Dirnagl U. Ischemia and stroke. Adv Exp Med Biol 2002;513:455–73. [PubMed: 12575832]
32. van Kooten F, Ciabattoni G, Patrono C, Dippel DW, Koudstaal PJ. Platelet activation and lipid peroxidation in patients with acute ischemic stroke. Stroke; a Journal Of Cerebral Circulation 1997;288:1557. [PubMed: 9259748]
33. Zhang W, Stanimirovic D, Hermann J, Gulati R, Napoli C, Woodrum JE, Lerman LO, Rodriguez-Porcel M, Sica V, Simari RD, Ciechanover A, Lerman A, Williams AJ, Hale SL, Moffett JR, Dave JR, Elliott PJ, Adams J, Tortella FC, Raghavendra Rao VL, Bowen KK, Dhodda VK, Song G, Franklin JL, Gavva NR, Dempsey RJ, Shah IM, Lees KR, Pien CP, Asai A, Tanahashi N, Qiu JH, Saito N, Chi S, Kawahara N, Tanaka K, Kirino T. Current and future therapeutic strategies to target inflammation in stroke. Current Drug Targets - Inflammation and Allergy 2002;12:151–66. [PubMed: 14561197]
34. Hall ED, Braughler JM. Central nervous system trauma and stroke. II. Physiological and pharmacological evidence for involvement of oxygen radicals and lipid peroxidation. Free Radical Biology & Medicine 1989;63:303–13. [PubMed: 2663663]
35. Chen Y, Zackert WE, Roberts LJ 2nd, Morrow JD. Evidence for the formation of a novel cyclopentenone isoprostane, 15-A2t-isoprostane (8-iso-prostaglandin A2) in vivo. Biochimica Et Biophysica Acta 1999;14363:550. [PubMed: 9989284]
36. Pisani A, Calabresi P, Tozzi A, D'Angelo V, Bernardi G, Iadecola C. L-Type Ca2+ channel blockers attenuate electrical changes and Ca2+ rise induced by oxygen/glucose deprivation in cortical neurons · Editorial Comment. Stroke 1998;291:196–202. [PubMed: 9445351]
37. Vornov JJ, Tasker RC, Coyle JT. Delayed protection by MK-801 and tetrodotoxin in a rat organotypic hippocampal culture model of ischemia. Stroke 1994;252:457–64. [PubMed: 8303757]discussion 464–5
38. Ehrenberg B, Montana V, Wei MD, Wuskell JP, Loew LM. Membrane potential can be determined in individual cells from the nernstian distribution of cationic dyes. Biophysical Journal 1988;535:785–794. [PubMed: 3390520]

39. Lipsky N, Pedersen P. Mitochondrial turnover in animal cells. Half-lives of mitochondria and mitochondrial subfractions of rat liver based on [14C]bicarbonate incorporation. Journal Of Biological Chemistry 1981;256:8652–8657. [PubMed: 7263675]
40. Haugland, R. Handbook of Fluorescent Probes and Research Chemicals. Molecular Probes Inc; 1999.
41. Hansford RG. Relation Between Mitochondrial Calcium-Transport And Control Of Energy-Metabolism. Reviews Of Physiology Biochemistry And Pharmacology 1985;102:1–72.
42. Halestrap AP. Calcium, mitochondria and reperfusion injury: a pore way to die. Biochemical Society Transactions 2006;34(Pt 2):232–7. [PubMed: 16545083]
43. Schild L, Reiser G. Oxidative stress is involved in the permeabilization of the inner membrane of brain mitochondria exposed to hypoxia/reoxygenation and low micromolar Ca2+ Febs Journal 2005;27214:3593–601. [PubMed: 16008559]
44. Friberg H, Wieloch T. Mitochondrial permeability transition in acute neurodegeneration. Biochimie 2002;842–3:241–50.
45. Javadov S, Karmazyn M. Mitochondrial permeability transition pore opening as an endpoint to initiate cell death and as a putative target for cardioprotection. Cellular Physiology and Biochemistry 2007;201–4:1–22.
46. Scorrano L, Penzo D, Petronilli V, Pagano F, Bernardi P. Arachidonic acid causes cell death through the mitochondrial permeability transition. Implications for tumor necrosis factor-alpha aopototic signaling. Journal of Biological Chemistry 2001;27615:12035–40. [PubMed: 11134037]
47. Murphy E, Steenbergen C. Preconditioning: The mitochondrial connection. Annual Review of Physiology 2007;691:51–67.
48. Nunez G, Benedict MA, Hu Y, Inohara N. Caspases: the proteases of the apoptotic pathway. Oncogene 1998;1725:3237–45. [PubMed: 9916986]
49. Sugawara T, Fujimura M, Morita-Fujimura Y, Kawase M, Chan PH. Mitochondrial release of cytochrome c corresponds to the selective vulnerability of hippocampal CA1 neurons in rats after transient global cerebral ischemia. Journal of Neuroscience 1999;1922:RC39. [PubMed: 10559429]
50. Hubatsch I, Mannervik B, Gao L, Roberts LJ, Chen Y, Morrow JD. The cyclopentenone product of lipid peroxidation, 15-A(2t)-isoprostane (8-isoprostaglandin A(2)), is efficiently conjugated with glutathione by human and rat glutathione transferase A4-4. Chemical Research in Toxicology 2002;159:1114–8. [PubMed: 12230403]
51. Montine KS, Quinn JF, Zhang J, Fessel JP, Roberts LJ 2nd, Morrow JD, Montine TJ. Isoprostanes and related products of lipid peroxidation in neurodegenerative diseases. Chemistry & Physics of Lipids 2004;1281–2:117–24.
52. Chan PH. Mitochondrial dysfunction and oxidative stress as determinants of cell death/survival in stroke. Annals of the New York Academy of Sciences 2005;10421:203–209. [PubMed: 15965064]
53. Vander Heiden MG, Chandel NS, Williamson EK, Schumacker PT, Thompson CB. Bcl-xL regulates the membrane potential and volume homeostasis of mitochondria. Cell 1997;91:627. [PubMed: 9393856]
54. Kennedy SG, Kandel ES, Cross TK, Hay N. Akt/Protein kinase B inhibits cell death by preventing the release of cytochrome c from mitochondria. Molecular and Cellular Biology 1999;198:5800–10. [PubMed: 10409766]
55. Scarlett JL, Sheard PW, Hughes G, Ledgerwood EC, Ku HH, Murphy MP. Changes in mitochondrial membrane potential during staurosporine-induced apoptosis in Jurkat cells. FEBS Letters 2000;4753:267–72. [PubMed: 10869569]
56. Kim H, Rafiuddin-Shah M, Tu HC, Jeffers JR, Zambetti GP, Hsieh JJ, Cheng EH. Hierarchical regulation of mitochondrion-dependent apoptosis by BCL-2 subfamilies. Nature Cell Biology 2006;812:1348–58.
57. Willis SN, Chen L, Dewson G, Wei A, Naik E, Fletcher JI, Adams JM, Huang DC. Proapoptotic Bak is sequestered by Mcl-1 and Bcl-xL, but not Bcl-2, until displaced by BH3-only proteins. Genes and Development 2005;1911:1294–305. [PubMed: 15901672]
58. Shroff EH, Snyder C, Chandel NS. Role of Bcl-2 family members in anoxia induced cell death. Cell Cycle 2007;67:807–9. [PubMed: 17377500]

59. Halestrap AP, Clarke SJ, Javadov SA. Mitochondrial permeability transition pore opening during myocardial reperfusion - a target for cardioprotection. Cardiovascular Research 2004;613:372–385. [PubMed: 14962470]

60. Zoratti M, Szabo I, De Marchi U. Mitochondrial permeability transitions: how many doors to the house? Biochimica et Biophysica Acta 2005;17061–2:40–52.

61. Bernardi P. The mitochondrial permeability transition from in vitro artifact to disease target. FEBS Journal 2006;273:2077. [PubMed: 16649987]

62. Halestrap AP, Woodfield KY, Connern CP. Oxidative stress, thiol reagents, and membrane potential modulate the mitochondrial permeability transition by affecting nucleotide binding to the adenine nucleotide translocase. Journal of Biological Chemistry 1997;2726:3346–54. [PubMed: 9013575]

63. McStay GP, Clarke SJ, Halestrap AP. Role of critical thiol groups on the matrix surface of the adenine nucleotide translocase in the mechanism of the mitochondrial permeability transition pore. Biochemical Journal 367Pt 2002;2:541–8.

64. Saito Y, Nishio K, Numakawa Y, Ogawa Y, Yoshida Y, Noguchi N, Niki E. Protective effects of 15-deoxy-Delta12,14-prostaglandin J2 against glutamate-induced cell death in primary cortical neuron cultures: induction of adaptive response and enhancement of cell tolerance primarily through up-regulation of cellular glutathione. J Neurochemistry 2007;1025:1625–34.

65. Cheng YD, Al-Khoury L, Zivin JA. Neuroprotection for Ischemic Stroke: Two Decades of Success and Failure. NeuroRx 2004;11:36–45. [PubMed: 15717006]

66. Kaduce TL, Chen Y, Hell JW, Spector AA. Docosahexaenoic acid synthesis from n-3 fatty acid precursors in rat hippocampal neurons. Journal of Neurochemistry 2008;1054:1525–35. [PubMed: 18248613]

67. Morrow JD. Is oxidant stress a connection between obesity and atherosclerosis? Arteriosclerosis, Thrombosis & Vascular Biology 2003;233:368–70.

68. Gross M, Steffes M, Jacobs DR Jr, Yu X, Lewis L, Lewis CE, Loria CM. Plasma F2-isoprostanes and coronary artery calcification: the CARDIA Study. Clinical Chemistry 2005;511:125–31. [PubMed: 15514100]

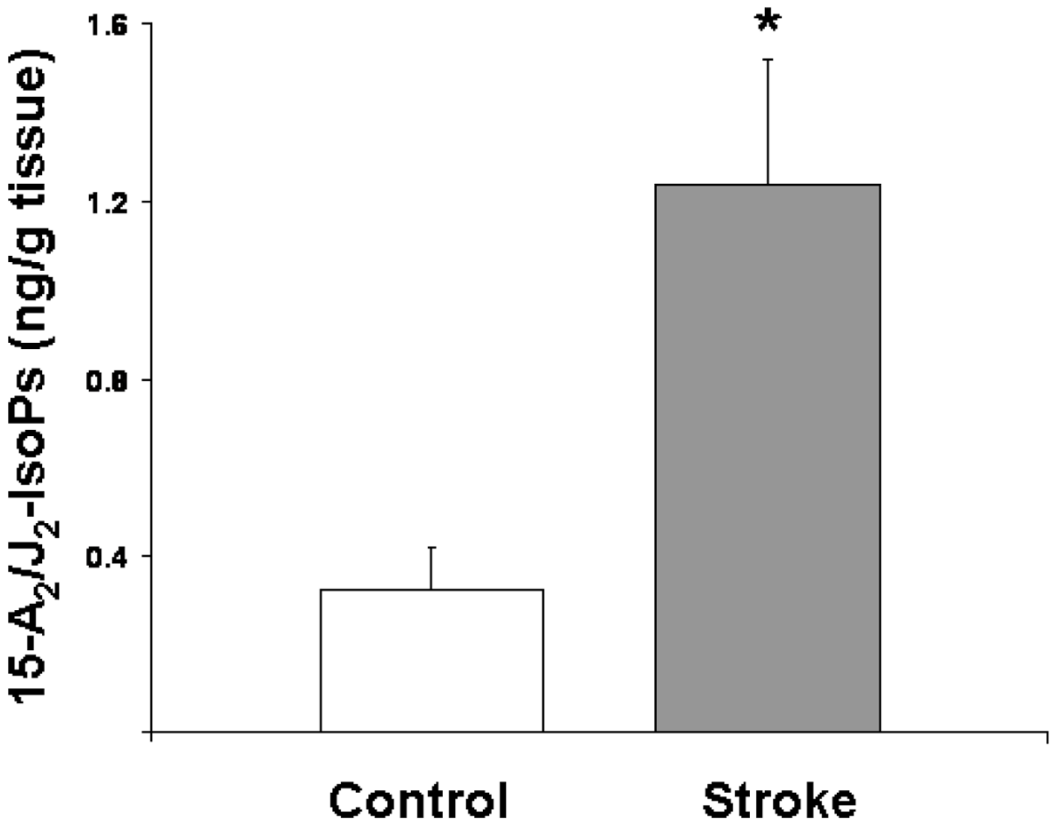

Fig. 1. Levels of esterified 15-A_2/J_2-IsoPs are increased in postmortem brain samples from human stroke patients

Post-mortem samples from cerebral cortex of ischemic stroke patient brains or control brains not exhibiting stroke were subjected to liquid chromatography tandem mass spectrometric analysis, and concentrations of membrane-esterified 15-A_2/J_2-IsoPs were quantified by stable isotope dilution using a deuterium-labeled PGA_2 internal standard. * denotes statistical significance compared to control sample as determined by two-tailed *t*-test with $p < 0.05$.

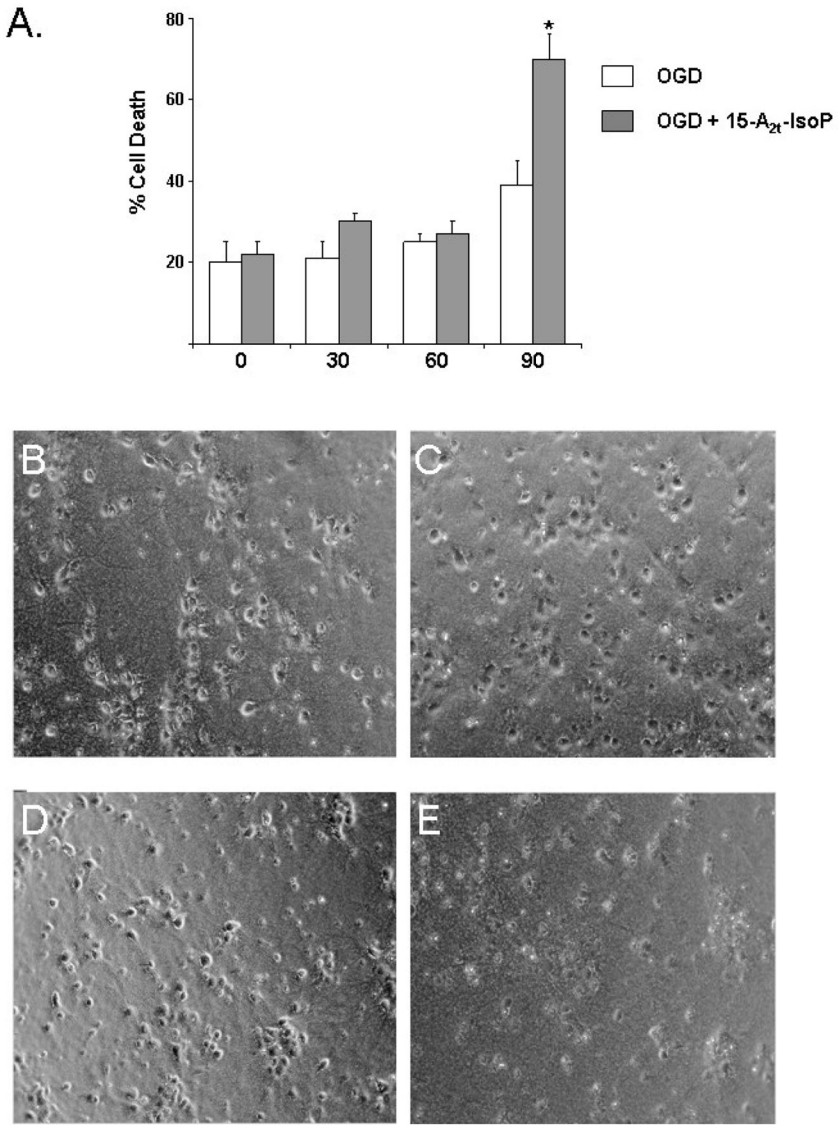

Fig. 2. 15-A_{2t}-IsoP potentiates ischemic injury

A) Exposure of neurons to prolonged oxygen glucose deprivation (OGD) led to increased cell death in the presence of 10μM 15-A_{2t}-IsoP. Data represent the mean of three independent experiments normalized to treatment which causes 100% cell death in this system ± S.E.M. * denotes statistical significance as compared to no OGD as determined by two-tailed *t*-test with $p<0.05$. Representative images of primary neuronal cultures which were incubated for 24 hours in 10μM DMSO (B) or 15-A_{2t}-IsoP (C) demonstrate many healthy phase bright neurons with an elaborate series of processes and well defined soma. Upon 90 minute ischemia (D), cytoarchitectural changes become more pronounced with cell soma shrinkage, loss of process integrity and some evidence in the upper right quadrant of highly pyknotic neurons. A dramatic loss of neurons was only evident following exposure to a combination of ischemia and 10μM 15-A_{2t}-IsoP (E).

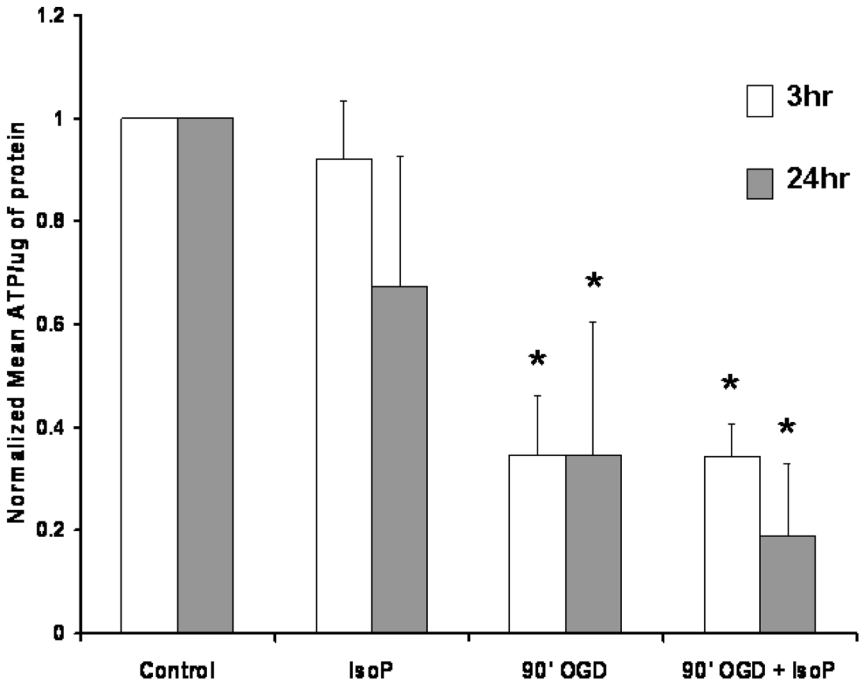

Fig. 3. 15-A_{2t}-IsoP treatment does not lead to decreased ATP content

ATP levels from neuronal cultures treated with DMSO (control) or 10μM 15-A_{2t}-IsoP were measured 3 (white) or 24 hrs (gray) following OGD. Data were normalized for total protein and are expressed as % control ± S.E.M from 3–5 independent experiments. * denotes statistical significance as compared to control as determined by two tail *t*-test with $p < 0.05$.

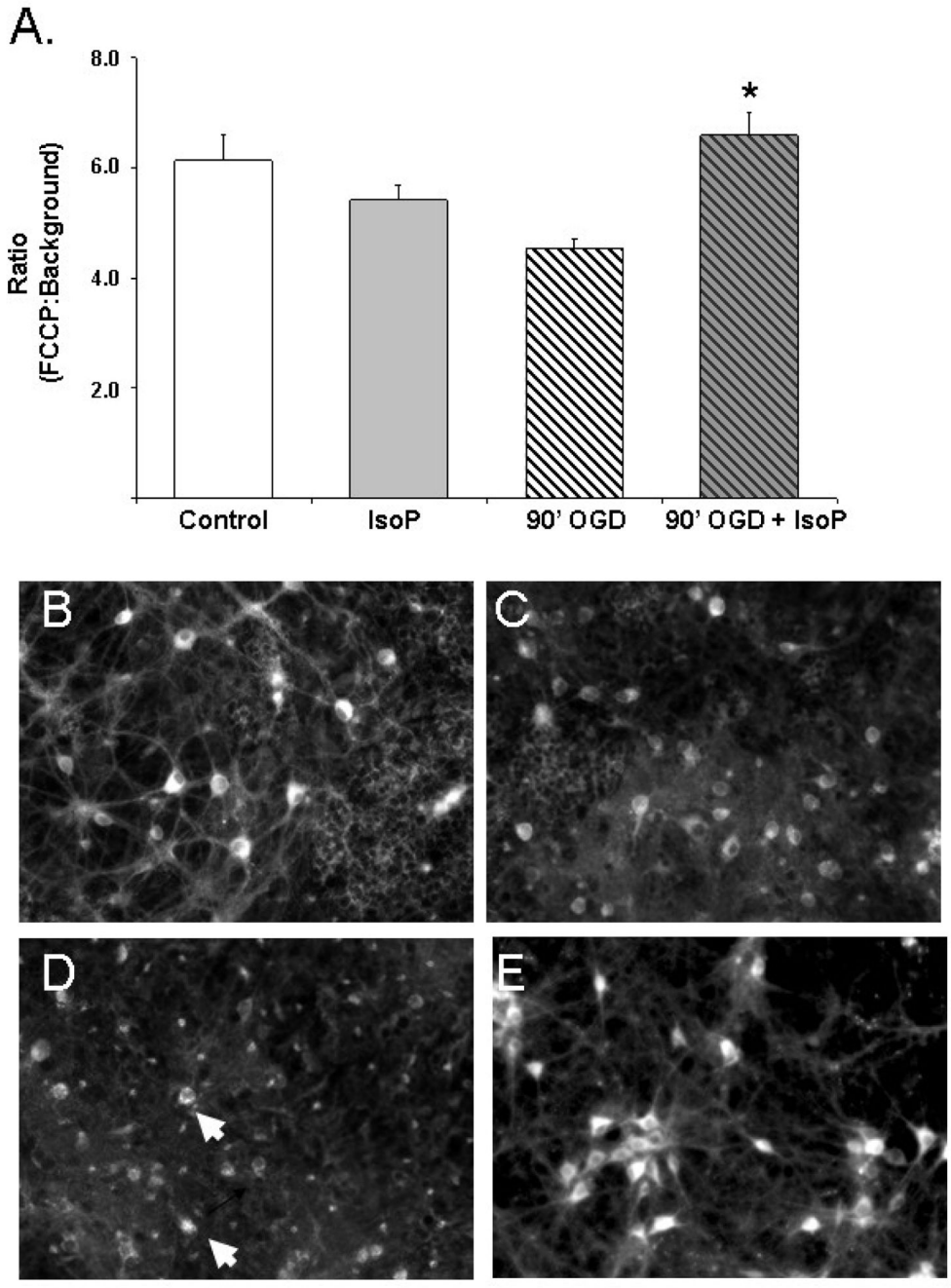

Fig. 4. 15-A_{2t}-IsoP alters mitochondrial membrane potential

A) The effects of 10μM 15-A_{2t}-IsoP exposure in the presence or absence of 90 minute OGD on mitochondrial membrane potential were evaluated by loading cells with 50nM TMRE for 20 minutes. Data represents the mean neuron pixel value ratio of FCCP signal to background ± S.E.M. of three independent experiments. The combination of OGD and IsoP increased mitochondrial polarity and TMRE intensity. This observation is demonstrated by representative photomicrographs from DMSO control (B), 10μM 15-A_{2t}-IsoP (C), 90 minute OGD (D), or a combination of OGD and 10μM 15-A_{2t}-IsoP (E). Both IsoP and OGD treatment resulted in loss of mitochondrial polarity in processes compared to controls. However, the

combination of OGD and IsoP increased uptake of TMRE with many intensely labeled neuronal cell bodies (arrows).

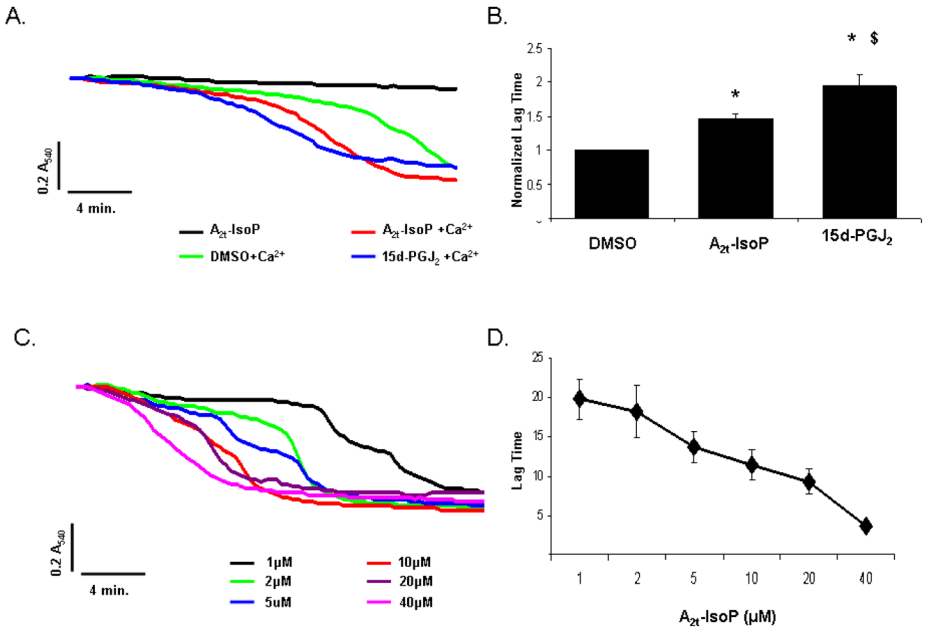

Fig. 5. 15-A_{2t}-IsoP enhances stress associated PTP pore opening

A) Purified mitochondria were incubated with 10μM DMSO, 15-A_{2t}-IsoP, or 15d-PGJ_2 in the absence or presence of Ca^{2+} and PTP opening was assessed by measuring alterations in absorbance over time. Data are from a representative experiment performed in duplicate. B) The average lag time to pore opening was measured by determining the maximal rate of change and normalized to DMSO with Ca^{2+} exposure. Data represent the normalized lag time ± S.E.M from four independent experiments. Statistical significance was determined by two-tailed *t*-test with $p < 0.05$ as compared to DMSO (*) or A_{2t}-IsoP ($). C) Dose response curves for IsoP induced PTP opening were performed using 1–40μM IsoP as shown in the representative experiment. D) The pooled data from three independent experiments ± S.E.M support a dose response relationship between PTP opening time and IsoP concentration.

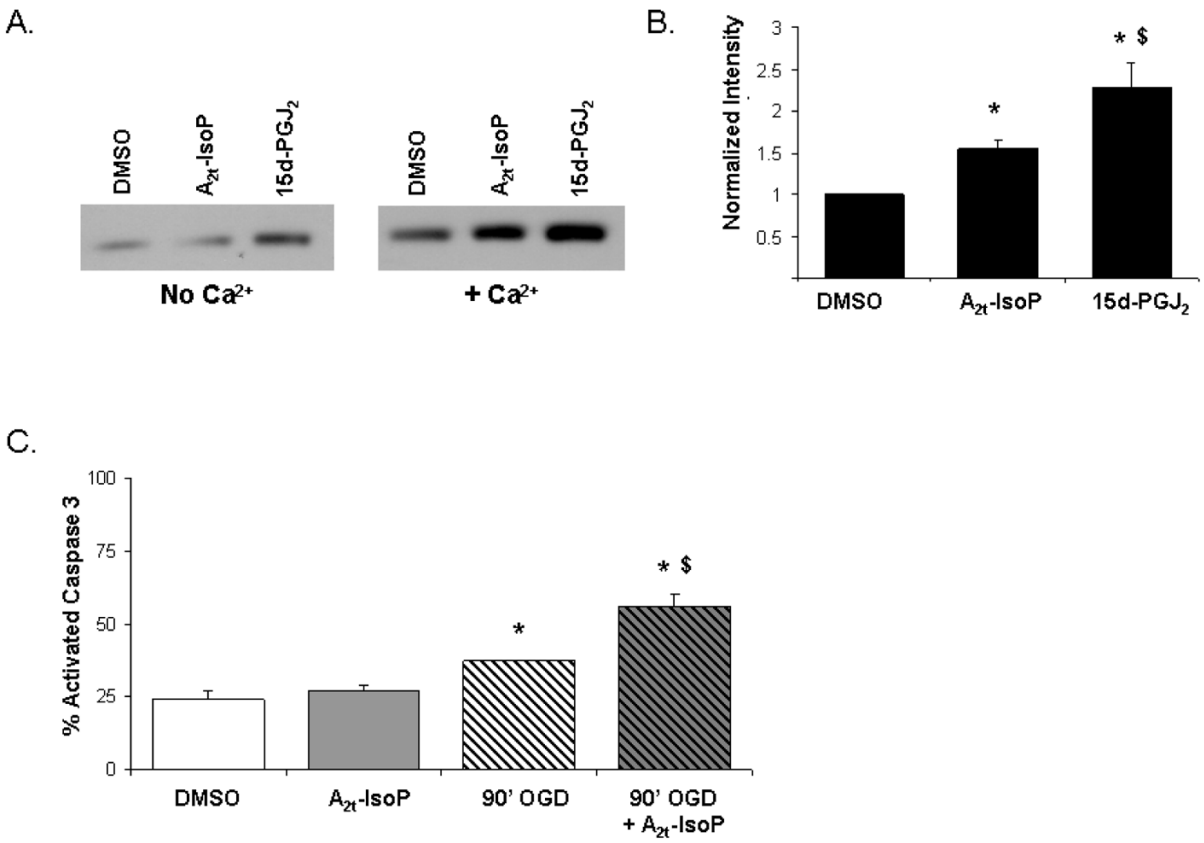

Fig. 6. 15-A_{2t}-IsoP exposure causes cytochrome *c* release from mitochondria and activates apoptotic pathways in combination with OGD

A) Cytochrome *c* release from the inner mitochondrial membrane was assessed from purified mitochondria incubated for five minutes with 10μM DMSO, 15-A_{2t}-IsoP, or 15d-PGJ_2 in the presence or absence of Ca^{2+}. Following the incubation, the supernatant was centrifugally separated from the organelle and cytochrome *c* release was analyzed by western blot. B) Quantification of cytochrome *c* using Image J analysis software revealed a 1.5 fold increase in cytochrome *c* release induced by 15-A_{2t}-IsoP and a 2-fold increase by15d-PGJ_2. Data represent the mean intensity normalized to DMSO with Ca^{2+} ± S.E.M for three independent experiments. Statistical significance was determined by two-tailed *t*-test with $p < 0.05$ as compared to DMSO (*) or 15-A_{2t}-IsoP ($). C) The combination of 90'OGD and IsoP exposure resulted in a significant increase in activated caspase 3 containing cells as compared to DMSO, 15-A_{2t}-IsoP or OGD alone 6 hours following exposure. Data represent the mean % of cells exhibiting activated caspase 3 for five different fields of views ± S.E.M from three independent experiments. Statistical significance was determined by two-tailed *t*-test with $p < 0.05$ as compared to DMSO (*) or 90'OGD ($).